

C500 Report

04/21/2006

**Quantum chemical modeling study of
AG vs. GA bifunctional binding of cisplatin**

Yogita Mantri

Advisor: Prof. Mu-Hyun Baik

Abstract

Cisplatin is one of the most widely used anti-cancer drugs. Its primary cellular target is genomic DNA to which it binds predominantly by forming an intra-strand crosslink between two adjacent purine bases. This bifunctional binding is thought to occur *via* initial formation of a monofunctional adduct followed by closure in the 5' or 3' direction. Experimental evidence suggests that the 5' direction is exclusively preferred. This study focuses on understanding this directional preference using high-level DFT models. Fully optimized bifunctional structures for the dinucleotides 5'dApG3' (AG) and 5'dGpA3' (GA) bound to cisplatin reveal that the AG adduct is lower in energy than GA by around 7 kcal/mol. The underlying electronic features that give rise to this thermodynamic difference of platinum binding were examined in detail. Surprisingly, we found that the puckering of the ribose rings plays an important role in determining the energetics of the bifunctional adducts.

Introduction

Cis-diamminedichloroplatinum(II) (Fig 1, *left*), *cisplatin*, is a potent anti-cancer drug which is widely used against a variety of cancers, in particular testicular cancer.² Although it was approved for use by the FDA in 1978, and is one of the most successful anti-cancer drugs, its use has been limited due to its severe side-effects.² Several other platinum-based drugs have been tested, but only a few among them have been approved for clinical use to date, namely carboplatin³⁰ and oxaliplatin²⁹. Despite its widespread

usage, many aspects of the cytotoxic mechanism of cisplatin are not fully understood. A better understanding of its cellular binding behavior and its effect on cell-survival may help in the rational design of better platinum-based drugs.

The anti-tumor activity of cisplatin was discovered accidentally during a study of the effect of an electric field on bacterial growth.³ Compounds formed by the reaction of the platinum electrodes with the ammonium chloride in the buffer stopped cell division and induced filamentous growth.³ These compounds were later tested on mice and found to exhibit anti-tumor activity, which eventually led to the FDA approval of cisplatin.

Cisplatin contains two labile chloride ligands in the *cis* position that function as leaving groups (Fig 1, *left*).⁴ These ligands remain bound to platinum in the plasma due to its high chloride concentration of around 100 mM. Once inside a cell, however, the sharply decreased *intracellular* chloride concentration of around 4 mM⁵ causes cisplatin to undergo hydrolysis, wherein the chloride ligands are substituted by aqua ligands to form the activated complexes $[\text{Pt}(\text{NH}_3)_2\text{Cl}(\text{H}_2\text{O})]^+$ and $[\text{Pt}(\text{NH}_3)_2(\text{H}_2\text{O})_2]^{2+}$ (Fig 1, *right*). These complexes then bind to various cellular components like DNA, RNA, proteins and membrane phospholipids.

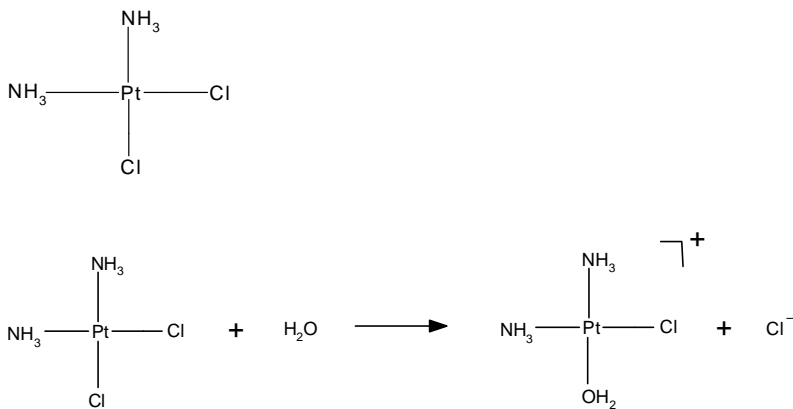


Figure 2. Types of cisplatin adducts²⁸

Goal of current study: Effect of Strand Orientation

As mentioned earlier, the most commonly seen cisplatin-DNA adduct is the bifunctional *intrastrand* adduct GpG, which is followed by ApG. However, an isomeric GpA adduct has never been observed in DNA. Experimental studies on a DNA sequence containing the trimer 5'ApGpA 3' have shown that after platination of the central guanine, ring-closure to form a bifunctional adduct favors formation of ApG adducts (Fig 3).¹⁶ Thus there is a preference for closure from the 3' end to the 5' end. Previous attempts to explain this preference suggested that the N7 of the adenine to the 5' end was at a shorter distance (3 Å) compared to that at the 3' end (5 Å). However this explanation failed to take into account any local distortion upon monofunctional binding.¹ In addition, 1,3-*intrastrand* crosslinks are relatively common binding motifs, suggesting that a reasoning based on Pt-N distance alone is not sufficient. This project aims to understand the structural details of this preference.

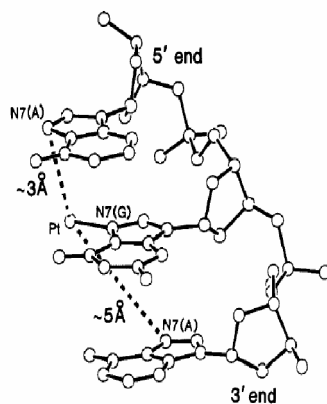


Figure 3.1 Bifunctional binding in AGA trimer

Methods

Computational Details:

All calculations were performed using the quantum mechanical package Jaguar 5.5^{17, 22} based on Density Functional Theory.^{18, 19} The basis sets used were B3LYP/6-31G**/LACVP + B3LYP/cc-pVTZ(-f)/LACV3P.^{23, 24, 25, 26} All energies were ZPE (unscaled freq.) corrected and entropy terms at T=298.15K were added. Solvation energies were computed using a continuum solvation model using water as the solvent.²⁷

I. Modeling of Platinated ApG and GpA nucleotides

Initial attempts were made to model the platinated bases as part of larger nucleotide chains such as trinucleotides (AGA, GAG), heptanucleotides (CCA*G*ACC, CCAG*A*CC) and double-stranded pentanucleotides. However, the larger structures were not stable in the gas phase and geometry optimizations either did not converge at all or gave extremely distorted structures. The most reasonable structures were dinucleotides BpB and pBpB (B=base, p=phosphate). The rest of the project focuses on comparisons among BpB-type structures.

II. Modeling of Platinated ApG and GpA dinucleotides

ApG and GpA dinucleotides (henceforth referred to as AG and GA, respectively) with cisplatin bifunctionally bound to their N7 atoms (Fig 4) were geometry optimized as

described above. The initial geometry guess was obtained by modifying cisplatin-bound DNA structures taken from the Protein Data Bank (PDB IDs: 1KSB²⁰, 1AIO³¹, 1A84³²). Both optimized structures starting from 1SKB were found to be lowest in energy, and were used for further analyses.

Results and discussion

The thermodynamic data for AG and GA pairs from all starting PDB structures follow experimental predictions, with AG being lower in energy than GA. The lowest energy pair starting from 1SKB was used for further analysis. The AG adduct is lower in energy than GA by around 7 kcal/mol, of which around 3 kcal/mol is attributed to electronic energy difference, and around 3.5 kcal/mol originates from solvation energy difference. (Table 1).

Table 1: Summary of thermodynamic data for GA and AG systems.

Type	$\Delta E(\text{SP})$ (eV)	ZPE 0 K (Kcal/ mol)	ΔH (eV)	Entropy 298.15 K (cal/mol K)	$T\Delta S$ at 298.15 k (Kcal/ mol)	ΔG gas (eV)	ΔG (Solv) (kcal/ mol)	$\Delta G(\text{Sol})$ (eV)	$\Delta\Delta G(\text{Sol})$ (kcal/ mol)
GA	- 74492. 634	362.19	- 74476. 928	246.76	73.57	- 74480. 118	- 186.57 74488. 209	-	
AG	- 74492.	361.62	- 74477.	248.60	74.12	- 74480.	- 190.11 74488.	-	

	767		085			300		544	
GA –	3.07	0.57	3.64	-1.84	-0.55	4.18	3.54	7.72	7.72
AG									
kcal/ mol									

Kinetically, GA has a higher activation barrier than AG, even though the monofunctional and transition state structures have lower energy for GA compared to AG (Fig 5). Thus, there is both a thermodynamic and kinetic preference for AG over GA.

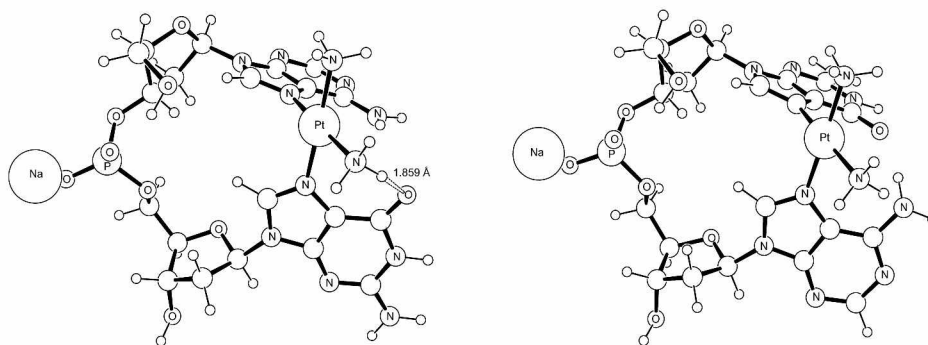


Figure 4. Optimized geometries of Platinated ApG and GpA

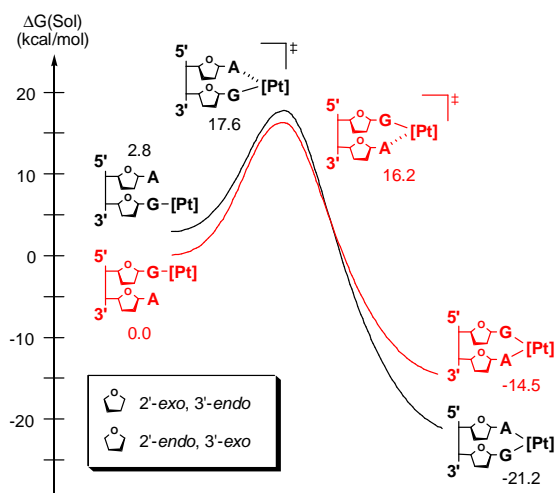


Figure 5. Reaction energy profile for AG and GA. Even though absolute energies for AG are higher than GA in monofunctional and transition state structures, the activation energy for AG (14.8 kcal/mol) is lower than GA (16.2 kcal/mol) by 1.4 kcal/mol.

Note: The bifunctional products shown above were modeled using one explicit water molecule as the leaving group, to keep monofunctional, transition state and bifunctional structures

Tracing the energy difference between AG and GA – Energy decomposition studies

Note: In the following sections [Pt] indicates the platinumdiammine species $\text{Pt}(\text{NH}_3)_2^{2+}$

The electronic energy difference of 3 kcal/mol is important, as it indicates an intrinsic preference for AG over GA that we must understand in greater detail. To derive such a deep conceptual understanding, we devised an energy decomposition protocol by systematically removing structural components of the model and comparing the energies of the smaller fragments. This “divide and conquer” approach is designed to reveal which portion of the molecule is responsible for the energy difference. In this case, the energy decomposition consisted of the following steps, starting from fully optimized dinucleotides (Fig 6):

- Compare energies of base + [Pt], i.e. removing sugar-phosphate backbones
- Compare energies of sugar-phosphate backbones
- Compare energies of dinucleotides without [Pt]
 - Removing one base
 - Removing one base + sugar
 - Removing base + sugar + phosphate

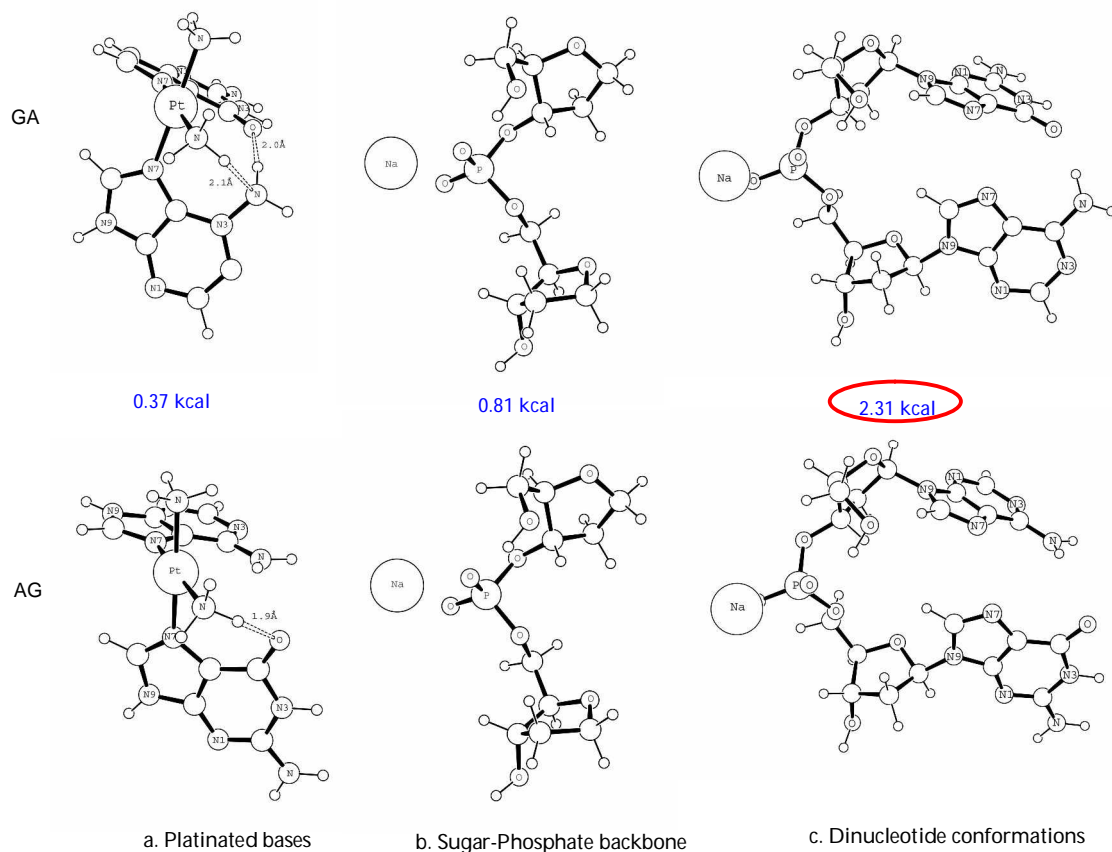


Figure 6. Comparison of fragments

Hypothesis 1: H-bond between O6 of 3' Guanine and NH₃ ligand of cisplatin

A strong hydrogen bond is present between the O6 of the 3' guanine and one of the NH₃ ligands of cisplatin. This hydrogen bond is absent in the GA dinucleotide due to the right-handedness of the DNA helix (Figure 6a). If this bond is responsible for the observed energy difference, it should be maintained in the fragment containing [Pt] with the two bases after removing the sugar-phosphate backbone. However, no energy difference is observed between the two structures, suggesting that the hydrogen bond does not have a differentiating contribution. This finding is in good agreement with an

experimental observation where the [Pt] unit was replaced by *N,N'*-dimethylpiperazine, which lacks NH groups, and was found to have the same conformation of the dinucleotide as the platinated model, suggesting that the hydrogen bonding between the O6 of guanine and the amine of cisplatin was not important.²¹

The sugar-phosphate backbone fragments are structurally almost superimposable and are only 0.8 kcal/mol apart (Figure 6b). Thus the possibility of backbone distortion leading to the energy difference can be ruled out.

The dinucleotide fragments of AG and GA after removing [Pt] differ in energy by 2.3 kcal/mol (Figure 6c). This means that most of the overall energy difference comes from the difference in these 2 structures. Since the backbone contribution is small, as seen from Figure 6b, the major contribution to the energy difference is the arrangement of the bases relative to the sugar-phosphate backbone.

The results lead to the conclusion that the [Pt] fragment has no direct electronic contribution to the observed energy difference in the final geometries. This is a surprising result and may suggest that there is nothing “special” about cisplatin binding, and the physical phenomenon of interest is generally valid for bifunctional substrate binding.

Hypothesis 2: Glycosidic bond length flexibility

As the overall energy difference can be reproduced by the fragments shown in Figure 6c, the non-platinated dinucleotides AG and GA were further analyzed and fragmented.

The glycosidic bond of the 5' base was found to be elongated to 1.501Å and 1.503Å for ApG and GpA respectively, compared to approximately 1.48 Å in natural DNA. Therefore smaller models were made to test the hypothesis that the energy

difference was due to the fact that adenine was intrinsically more flexible than guanine, thus leading to a more stable structure even with an elongated glycosidic bond. This, however, is not the case, since the energy difference is maintained when the glycosidic bond lengths are changed. Thus the bond length has only a negligible contribution.

Since the two dinucleotides are almost perfectly superimposable, the next step was to further fragment the structures by removing one base at a time, followed by the sugar-phosphate backbone (Fig 7).

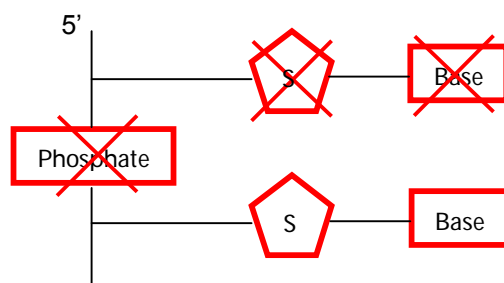


Figure 7. Successive removal of components

Isodesmic energy comparison

Energy comparison between adenine and guanine containing structures was carried out by subtracting the difference between free adenine and guanine from the difference in the two structures, thus keeping the comparison mass-balanced. The results are summarized in Fig 8 below.

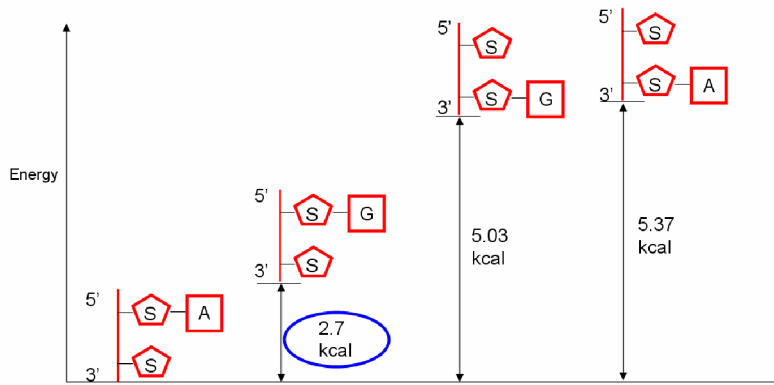


Figure 8. Comparison of fragments after removing one base

The energy profile shown above leads to the following conclusions:

- The 3' bases do not contribute to the energy difference since they are almost identical.
- The 5' bases can reproduce the energy difference between AG and GA dinucleotides, and thus may be solely responsible for the overall energy difference.

Hypothesis 3: 3'-endo sugar pucker more favorable for adenine

The 5' bases undergo a conformational transformation of the sugar pucker upon platinum binding from 2'-endo to 3'-endo. This enables the 5' base to bind to the platinum below it, by making it axial. The 3' sugar may or may not change its pucker upon platination, and appears to contribute to bifunctional binding by bending upwards towards the platinum above it.

To test this hypothesis, further fragmentation was carried out, successively reducing the model to a nucleotide and finally to a nucleoside. The results are somewhat ambiguous and some aspects of the relative energies do not match the profile above.

Further work is currently ongoing. One consistent feature is the energy difference of approximately 2.5 kcal/mol between the 5' sugars with 3'-*endo* pucker attached to guanine and adenine.

Thus, the conclusion so far is that the differences in formation of AG and GA are due to intrinsic preferences for a particular type of sugar puckering and are not directly the result of the cisplatin unit itself, as evident from Figures 6 and 8.

Future work

Some of the inconsistencies in the data must be resolved. Diverse fragmentation strategies are being pursued, in addition to varying technical parameters to ensure that the computed results are not numerical artifacts. Another possible approach being considered is to simplify dinucleotides to purines and sequentially add the functional group to trace the energy contributions. Finally, the transition state for bifunctional closure will be reoptimized by modeling the sugar pucker switch, as we had not paid enough attention to this feature in our initial approach.

A detailed kinetic profile will be mapped by considering all possibilities including sugar pucker switching before and after the platination step. Since it still holds that the observed preference for one conformer over another has little to do with the actual species forming the adducts and more to do with which distortions are actually allowed energetically, it seems reasonable to propose a generic mechanism for formation of these bifunctional adducts via sugar pucker switching, and use other bifunctionally binding

species to validate these claims. Some examples could include oxaliplatin (Fig 9) and melphalan, a nitrogen mustard (Fig 10).

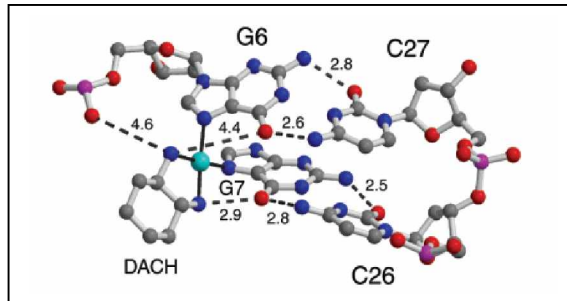


Figure 9. GpG bifunctional adduct by Oxaliplatin (DACH)²⁹

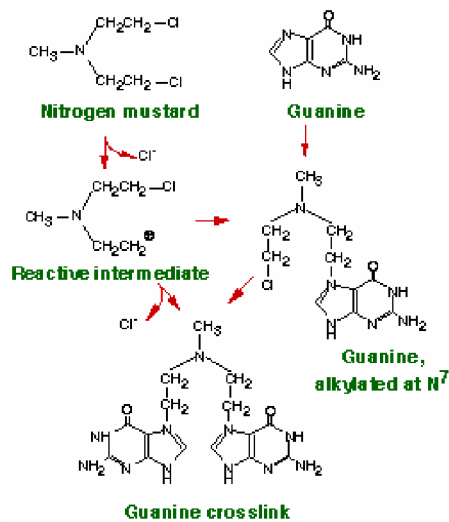


Figure 10. Schematic of bifunctional binding by Nitrogen Mustards

http://www.ovc.uoguelph.ca/BioMed/Courses/Public/Pharmacology/pharmsite/98-409/Cancer/Anticancer_drugs1.html#Nitrog_Must

References

1. Dewan, J. C., *J. Am. Chem. Soc.* **1984**, *106*, 7239-7244.
2. Reedijk, J.; Lohman, P. H. M., *Pharmaceutisch Weekblad-Scientific Edition* **1985**, *7*, 173-180.
3. Rosenberg, B.; Van Camp, L.; Trosko, J. E.; Mansour, V. H., *Nature* **1969**, *222*, 385-386.
4. Tullius, T. D.; Ushay, H. M.; Merkel, C. M.; Caradonna, J. P.; Lippard, S. J., *ACS Symp. Ser.* **1983**, *209*, 51-74.
5. Lim, M. C.; Martin, R. B., *Journal of Inorganic & Nuclear Chemistry* **1976**, *38*, 1911-1914.
6. Harder, H. C.; Rosenber.B, *Int. J. Cancer* **1970**, *6*, 207-&.
7. Howle, J. A.; Gale, G. R., *Biochem. Pharmacol.* **1970**, *19*, 2757-&.
8. Baik, M. H.; Friesner, R. A.; Lippard, S. J., *J. Am. Chem. Soc.* **2003**, *125*, 14082-14092.
9. Sherman, S. E.; Gibson, D.; Wang, A. H. J.; Lippard, S. J., *J. Am. Chem. Soc.* **1988**, *110*, 7368-7381.
10. Bowler, B. E.; Lippard, S. J., *Biochemistry* **1986**, *25*, 3031-3038.
11. Malinge, J. M.; Schwartz, A.; Leng, M., *Nucleic Acids Res.* **1987**, *15*, 1779-1797.
12. Vanhemelryck, B.; Girault, J. P.; Chottard, G.; Valadon, P.; Laoui, A.; Chottard, J. C., *Inorg. Chem.* **1987**, *26*, 787-795.
13. Inagaki, K.; Kidani, Y., *Inorganica Chimica Acta-Bioinorganic Chemistry* **1983**, *80*, 171-176.

14. Zamble, D. B.; Mu, D.; Reardon, J. T.; Sancar, A.; Lippard, S. J., *Biochemistry* **1996**, *35*, 10004-10013.
15. Zamble, D. B.; Lippard, S. J., *Trends Biochem. Sci.* **1995**, *20*, 435-439.
16. Vanderveer, J. L.; Vandenberg, H.; Denhartog, J. H. J.; Fichtingerschepman, A. M. J.; Reedijk, J., *Inorg. Chem.* **1986**, *25*, 4657-4663.
17. Bachrach, S. M., *J. Am. Chem. Soc.* **2004**, *126*, 5018-5018.
18. Baerends, E. J.; Gritsenko, O. V., *J. Phys. Chem. A* **1997**, *101*, 5383-5403.
19. Kohn, W.; Becke, A. D.; Parr, R. G., *J. Phys. Chem.* **1996**, *100*, 12974-12980.
20. Marzilli, L. G.; Saad, J. S.; Kuklenyik, Z.; Keating, K. A.; Xu, Y. H., *J. Am. Chem. Soc.* **2001**, *123*, 2764-2770.
21. Sullivan, S. T.; Ciccarese, A.; Fanizzi, F. P.; Marzilli, L. G., *J. Am. Chem. Soc.* **2001**, *123*, 9345-9355.
22. *Schrödinger, Inc.*; Portland, Oregon, **2003**.
23. Becke, A. D. *J. Chem. Phys.* **1993**, *98*, 5648.
24. Lee, C. T.; Yang, W. T.; Parr, R. G. *Phys. Rev. B.* **1988**, *37*, 785.
25. Hay, P. J.; Wadt, W. R. *J. Chem. Phys.* **1985**, *82*, 270.
26. Dunning, T. H. *J. Chem. Phys.* **1989**, *90*, 1007.
27. Marten, B.; Kim, K.; Cortis, C.; Friesner, R. A.; Murphy, R. B.; Ringnalda, M. N.; Sitkoff, D.; Honig, B. *J. Phys. Chem.* **1996**, *100*, 11775
28. Sherman, S. E.; Lippard, S. J. *Chem. Rev.* **1987**, *87*, 1153-1181
29. Spingler, B., Whittington, D.A., Lippard, S.J. *Inorg.Chem.* **2001**, *40*, 5596-5602
30. Reedijk, J. *Chem. Commun.* **1996**, 801-806.

31. Takahara, P.M., Rosenzweig, A.C., Frederick, C.A., Lippard, S.J. *Nature* **1995**, 377
649-652.
32. Gelasco, A., Lippard, S.J. *Biochemistry*, **1998**, 37, 9230-9239.